

References and Notes

- (1) Thomas, J. K. *The Chemistry of Excitation at Interfaces*; ACS Monograph Series 181; American Chemical Society: Washington, DC, 1984.
- (2) Fendler, J. *Membrane Mimetic Chemistry*; Academic: New York, 1983.
- (3) Turro, N. J.; Grätzel, M.; Braun, A. M. *Angew. Chem., Int. Ed. Engl.* **1980**, *19*, 675.
- (4) Setton, R. In *Chemical Reactions in Organic and Inorganic Constrained Systems*; Nato ASI Series C; D. Reidel: New York, 1985; Vol. 165.
- (5) Strauss, U. P.; Gershfeld, N. L. *J. Phys. Chem.* **1954**, *58*, 747. Strauss, U. P.; Gershfeld, N. L.; Crook, E. H. *Ibid.* **1956**, *60*, 577; *Polymer Prepr.* **1986**, *27*(1) 425.
- (6) (a) Wang, K. H.; Kimura, K.; Smid, J. *J. Polym. Chem.* **1983**, *21*(2) 579. (b) Roland, B.; Kimura, K.; Smid, J. *J. Colloid Interf. Sci.* **1984**, *97*(2), 392. (c) Roland, B.; Smid, J. *J. Am. Chem. Soc.* **1983**, *105*, 5269.
- (7) Geacintov, N. E.; Prusic, T.; Khosroffian, J. *J. Am. Chem. Soc.* **1976**, *98*, 6444 and references therein.
- (8) Strauss, U. P. In *Microdomains in Polymer Solutions*; Dubin, P., Ed.; Plenum: New York, 1985; pp 1-12.
- (9) Sugai, S.; Nitta, K.; Ohno, N. In *Microdomains in Polymer Solutions*; Dubin, P., Ed.; Plenum: New York, 1985; pp 13-32.
- (10) Nakahira, T.; Grätzel, M. *Macromol. Chem. Rapid Commun.* **1985**, *6*, 341.
- (11) (a) Chu, D. Y.; Thomas, J. K. *Macromolecules* **1984**, *17*, 2142. (b) Chu, D. Y.; Thomas, J. K. *J. Phys. Chem.* **1985**, *89*, 4065. (c) Chu, D. Y.; Thomas, J. K. *J. Am. Chem. Soc.* **1986**, *108*, 6270.
- (12) (a) Shinitzky, M.; Dianoux, A. C.; Gitler, C.; Weber, G. *Biochemistry* **1971**, *10*, 2106. (b) Grätzel, M.; Thomas, J. K. *J. Am. Chem. Soc.* **1973**, *95*, 6885. (c) Azumi, T.; McGlynn, S. P. *J. Chem. Phys.* **1962**, *37*, 2413.
- (13) Hashimoto, S.; Thomas, J. K. *J. Phys. Chem.* **1985**, *89*, 2771.
- (14) Kalyanasundaram, K.; Thomas, J. K. *J. Am. Chem. Soc.* **1977**, *99*, 2039.
- (15) Nakamura, T.; Thomas, J. K. *Langmuir* **1985**, *1*, 568.
- (16) Chen, T.; Thomas, J. K. *J. Polym. Sci., A-1* **1979**, *17*, 1103.
- (17) Katusin-Razem, B.; Wong, M.; Thomas, J. K. *J. Am. Chem. Soc.* **1978**, *100*, 1679.
- (18) (a) Heinzelmann, W.; Labhart, H. *Chem. Phys. Lett.* **1969**, *4*, 20. (b) Jagur-Grodzinski, J.; Feld, M.; Yang, S. L.; Szwarc, M. *J. Phys. Chem.* **1965**, *69*, 628. (c) Schomburg, H.; Steark, H.; Weller, A. *Chem. Phys. Lett.* **1973**, *21*, 433.
- (19) (a) Birks, J. B. *Photophysics of Aromatic Molecules*; Wiley-Interscience: New York, 1970; p 429. (b) Mataga, N.; Okada, T.; Yamamoto, N. *Bull. Chem. Soc. Jpn.* **1966**, *39*, 2562; *Chem. Phys. Lett.* **1967**, *1*, 119.
- (20) Reference 19(a), p 479.
- (21) Turro, N. J.; Yekta, L. A. *J. Am. Chem. Soc.* **1958**, *100*, 5951.
- (22) Reference 1, p 172.
- (23) Fendler, J. H.; Fendler, E. J. *Catalyst in Micellar and Macromolecular Systems*; Academic: New York, 1975.
- (24) (a) Tachiya, M. *Chem. Phys. Lett.* **1975**, *33*, 289; *J. Chem. Phys.* **1982**, *76*, 340. (b) Atik, S. S.; Singer, L. A. *Chem. Phys. Lett.* **1978**, *59*, 519.
- (25) (a) Hashimoto, S.; Thomas, J. K. *J. Am. Chem. Soc.* **1985**, *107*, 4655. (b) Nakajima, A. *Bull. Chem. Soc. Jpn.* **1984**, *57*, 1143 and references therein.
- (26) Almgren, M.; Grieser, F.; Thomas, J. K. *J. Am. Chem. Soc.* **1979**, *101*, 279.

Regime Transitions in Fractions of *cis*-Polyisoprene

P. J. Phillips* and N. Vatansever

Department of Materials Science and Engineering, The University of Tennessee, Knoxville, Tennessee 37996-2200. Received October 15, 1986

ABSTRACT: Relatively narrow fractions of *cis*-polyisoprene have been prepared from hevea rubber by nonsolvent precipitation. Following molecular weight characterization by intrinsic viscosity and gel permeation chromatography, crystallization studies were conducted using osmium tetroxide staining followed by transmission electron microscopy. Kinetic curves are typically bell shaped, the rate of crystal growth decreasing as molecular weight is increased. Secondary nucleation analyses show that the regime II-regime III transition occurs for fractions of lower molecular weight but that generally only regime III growth can be easily observed for molecular weights of 897 000 and above. Narrow fractions show a ratio of slopes for regime III to regime II close to 2.0 as predicted by theory whereas unfractionated systems give lower values (e.g., 1.65 for *cis*-polyisoprene from hevea rubber). Detailed studies of a fraction of molecular weight 313 000 show an extremely distorted bell-shaped crystallization curve. Kinetic analyses of the data demonstrate clearly the presence of all three crystallization regimes for the first time in any polymer. Morphological studies confirm the presence of a regime I-regime II transition. A major increase in branching occurs at temperatures just below that transition, as in polyethylene. The regime I region is characterized by molecular weight fractionation manifest by the concurrent presence of both axialites and single crystals with grossly different growth rates. This experimentation provides the first clear evidence for regime theory as currently developed.

Introduction

Recent major advances in our understanding of quiescent crystallization in polymers have resulted from the discovery of different regimes of nucleation. Prior to this advance it was generally assumed that nucleation on a crystal surface was always the rate-controlling event in lamellar growth.¹ The suggestion of a transition as a function of temperature and molecular weight from a situation where the nucleation rate was considerably slower than the rate of lateral spreading (regime I) to a condition where the two rates are comparable (regime II) was made by Lauritzen and Hoffman² in 1973. Experimental confirmation of this transition in narrow fractions of linear polyethylene followed shortly thereafter.³ It has now been

demonstrated⁴ that the effect can be observed in bulk crystallization of the unfractionated polymer and that the pressure dependence of the transition follows that of the equilibrium melting point. Only one other polymer is believed to show a similar regime transition⁵ although poly(ϵ -caprolactone) shows such an effect with time presumably due to a less narrow molecular weight distribution than polyethylene.⁶

The prediction of a second transition at even lower supercoolings, from regime II to regime III, was first made by Phillips in 1979⁷ and an appropriate theory was formulated by Hoffman in 1983.⁸ Such a transition is now believed to occur in several polymers including *cis*-polyisoprene,^{9,10} polypropylene,¹¹ and poly(phenylene sulfide).¹² Studies of the regime II-regime III transition analogous to those of the regime I-regime II transition in polyethylene as a function of molecular weight and temperature

* To whom all correspondence should be addressed.

Table I
Molecular Weight Data for Fractions

fraction	wt, g	$[\eta]$	M_v	M_w/M_n
1	0.1208	6.53	1.12×10^6	
2	0.0300			
3	0.2133	5.50	8.97×10^5	
4	0.1970	4.30	6.57×10^5	
5	0.1460	3.90	5.8×10^5	
6	0.3392	2.62	3.51×10^5	1.34
7	1.0832	3.85	5.71×10^5	
8	2.6361	3.70	5.43×10^5	
9	0.4103	2.39	3.13×10^5	1.58
10	1.3656	0.99	1.02×10^5	1.75
A ^a		7.91	1.42×10^6	

^a Obtained in separate fractionation experiment.

have not yet been reported for any system. Studies of poly(phenylene sulfide),¹² while considering two molecular weights and providing important data, did not produce conclusive analyses. In this paper we will report the results of a study of fractions of *cis*-polyisoprene ranging in molecular weight from 3×10^5 to 1.4×10^6 over the crystallization temperature range -40 to $+3$ °C, which demonstrate the existence of regimes I, II, and III in *cis*-polyisoprene. This research is the first such study for any polymer.

Experimental Section

Hevea rubber in the form of pale crepe was supplied by the Malaysian Rubber Board. It was purified by acetone extraction in a Soxhlet for 24 h to remove any soluble organics. Following drying, the remaining material was dissolved in hexane and filtered to remove gel fractions as high as 60% of the total mass.

Fractionation was carried out by using a 0.05% solution in hexane at 26 °C and dropwise addition of the nonsolvent 1-propanol under nitrogen and in the dark. Individual fractions were collected as listed in Table I. In each case the precipitated polymer was allowed to sediment for 12–48 h, dependent on fraction, before removal and collection. Fractions were collected after siphoning of the supernatant liquid, dissolved in hexane, reprecipitated, and dried to constant weight at room temperature *in vacuo*.

Viscosity-average molecular weights were determined by using a Cannon-Ubbelohde viscometer on THF solutions at 25 °C. Mark-Houwink equation constants $K = 1.09 \times 10^{-4}$ and $\alpha = 0.79$ ¹³ were used. Gel permeation chromatography was carried out by using THF solutions and a Waters Associates instrument, with styragel columns. Calibration was carried out by using narrow fractions of polystyrene.

Specimens for crystallization studies were prepared by film casting from a 2% hexane solution onto a water surface, an appropriate film thickness of ca. 800 Å being judged by a gold interference color in the film.¹⁴ Films were collected on 400-mesh copper electron microscope grids and dried in a vacuum for 20 min prior to crystallization which was carried out in a freezer. After the chosen time of crystallization, samples were stained with osmium tetroxide vapor for 20 s prior to examination in a Philips 300 or JEOL 200 CX transmission electron microscope. Unfortunately specimens of the lowest molecular weight (1×10^5) were mechanically unstable.

Results

Earlier studies have demonstrated that major nucleation of spherulites occurs at one and the same time for natural rubbers even though the nucleating species are smaller than the lamellar thickness and undetectable. The fractions studied here are no different. Growth rates were determined by using the well-established procedure for measuring the maximum lamellar length (i.e., larger spherulites present in the film) for chosen times at each crystallization temperature. Linear growth rates always resulted, as they did for unfractionated rubbers (for example, see Figure 1). All molecular weight fractions ex-

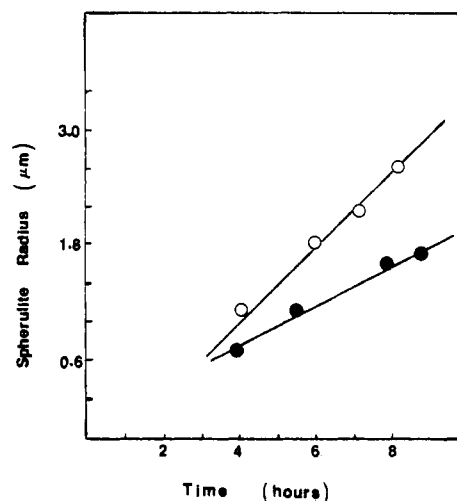


Figure 1. Lamellar growth of hevea rubber fractions with molecular weights (○) 3.13×10^5 and (●) 1.42×10^6 at -20 °C.

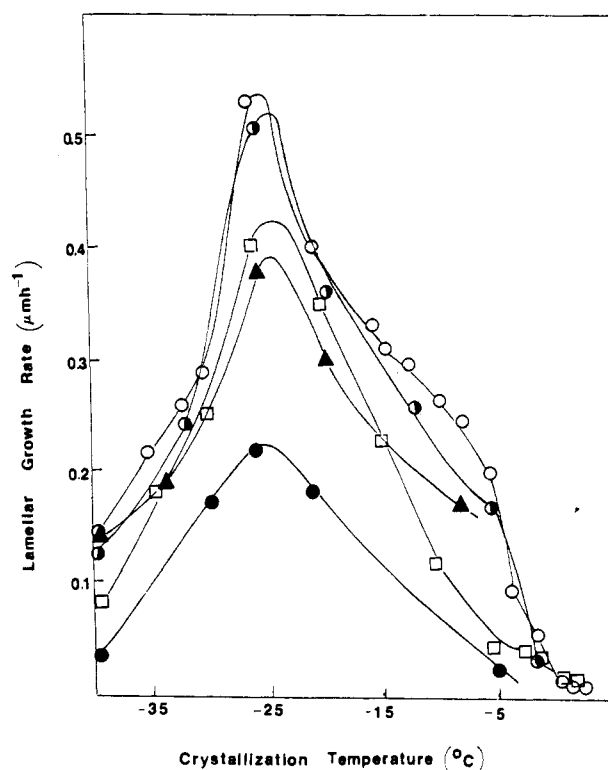


Figure 2. Lamellar growth rate vs. crystallization temperature for hevea rubber fractions with molecular weights (○) 3.13×10^5 , (●) 3.51×10^5 , (□) 5.43×10^5 , (▲) 8.97×10^5 , (●) 1.42×10^6 .

hibited bell-shaped curves which were not of identical or uniform shapes (Figure 2). The general trend of increasing molecular weight was to reduce the growth rate without influencing the temperature of the maximum growth rate. Similar behavior has been observed in a number of polymers, two examples being poly(tetramethyl-*p*-silphenylenesiloxane)¹⁵ and poly(ethylene terephthalate).¹⁶ The higher molecular weight fractions show more uniformly shaped curves, the two lowest molecular weight fractions showing changes in shape in the vicinity of -30 and -20 °C. Abnormally low rates of growth are apparent for the 5.43×10^5 molecular weight sample at low supercoolings. In this region it exhibits a growth rate lower than that of the 8.97×10^5 fraction. It is of course possible that the latter fraction is exhibiting an abnormally high growth rate which it also shows at high supercoolings. These effects could be caused by the molecular weight distributions

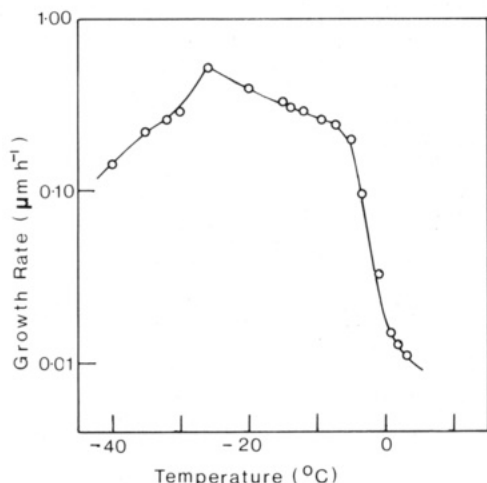


Figure 3. Lamellar growth curve of *cis*-polyisoprene of molecular weight 3.13×10^5 .

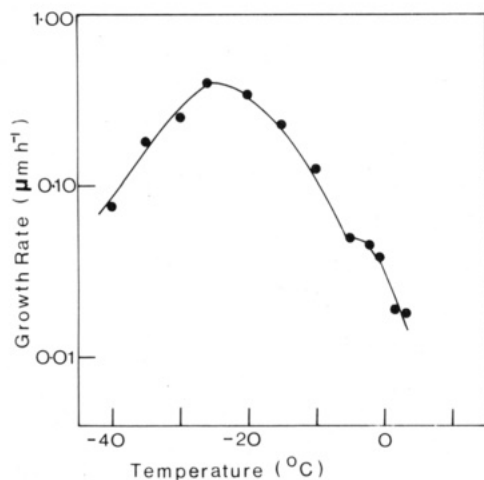


Figure 4. Lamellar growth curve of *cis*-polyisoprene of molecular weight 5.43×10^5 .

being broader than those of the lower molecular weight fractions. The two lower molecular weight fractions show distinct shoulders at low supercoolings. Unfortunately samples of molecular weight half a million and above could not be studied by using gel permeation chromatography due to clogging of the column. In the above studies little attention was paid to the regions of low supercooling because of the very long times needed in such studies. In order to better understand the nonuniformity of the bell-shaped curves, additional points were obtained for the fractions of molecular weight 313 000 and 543 000. Results are shown in Figures 3 and 4 by using a logarithm of growth rate vs. temperature plot to accentuate the low supercooling data. It can be seen that a very specific and unusual growth curve exists for the fraction of molecular weight 313 000.

Significant morphological changes were also observed. Above -8°C two different morphological species could be detected (Figure 5). First, large skeletalized single crystals occurred¹⁷ such as have been reported earlier for unfractionated polymer undergoing elevated pressure crystallization. The population density of this species increases as crystallization temperature is increased, becoming dominant for crystallization temperatures in excess of 3°C . Second, spherulite-like species that exhibit a platelet growth, as opposed to a ribbon-like growth, occur for lamellae in the "side-on", as opposed to "edge-on", orientation. It is believed that these objects are axialites, such as have already been observed in *trans*-polyisoprene.¹⁸ It

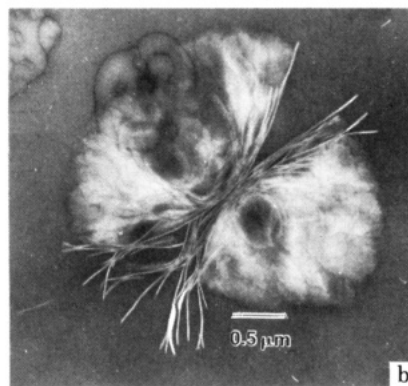
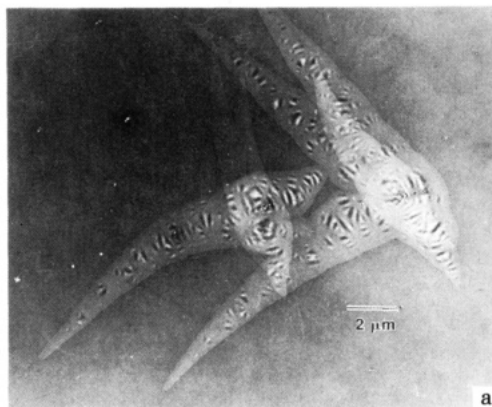


Figure 5. (a) Single crystals and (b) axialites in a fraction of molecular weight 3.13×10^5 grown in the regime I region.

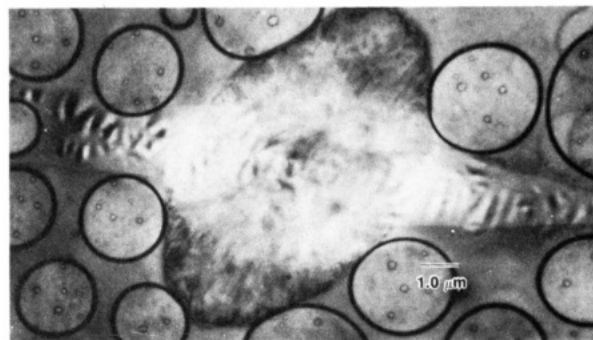


Figure 6. Conucleated single crystal and axialite grown at $+1.8^\circ\text{C}$.

is the growth rate of these species that was used in Figure 3 for linear growth rates above -8°C . Occasional species have been observed combining a single crystal and an axialite (Figure 6). Such objects clearly have nucleated together.

Studies of lamellar thickness were also carried out by using the electron micrographs, care being taken to ensure that values corresponded to the completely edge-on orientation. As in unfractionated *cis*-polyisoprenes the lamellar thickness distribution is generally narrow and the most probable lamellar thickness can be determined to within an error of $\pm 5 \text{ \AA}$ in these stained samples because of the combination of known lamellar orientation and sharp interfaces. The narrow distribution is known to be a result of the lack of any important thickening process.¹⁹ Some characteristic histograms of lamellar thickness distribution are shown in Figure 7. Data typical of medium supercoolings (part a) show narrow distributions. Care was taken at low supercoolings since it was possible that some thickening might occur in the axialitic region. Such data are presented in parts c and d where it can be seen that

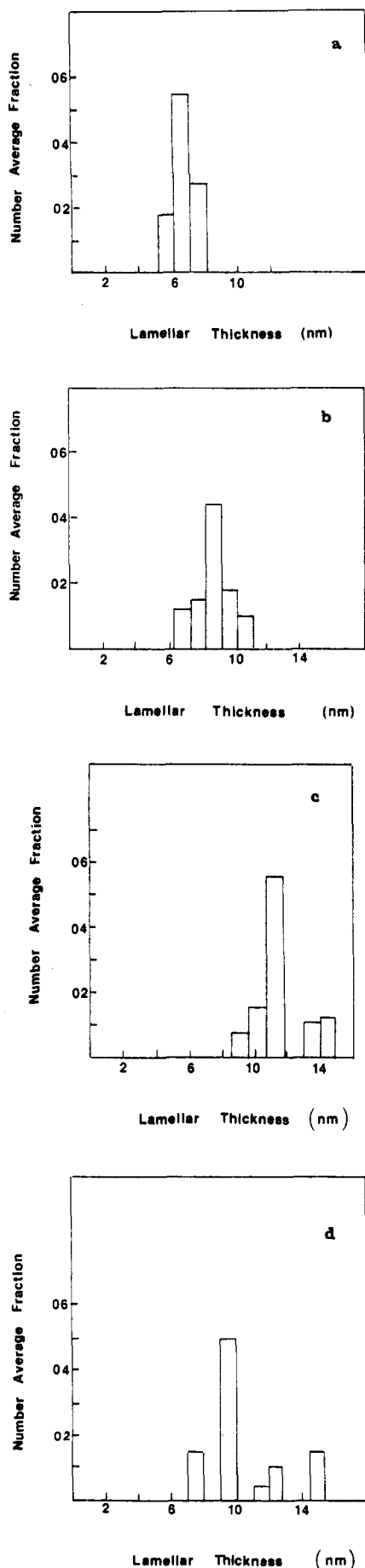


Figure 7. Histograms of lamellar thickness for (a) 3.13×10^5 at -26°C , (b) 5.43×10^5 at -0.6°C , (c) 3.13×10^5 at $+1.8^\circ\text{C}$, and (d) 5.43×10^5 at 1.4°C .

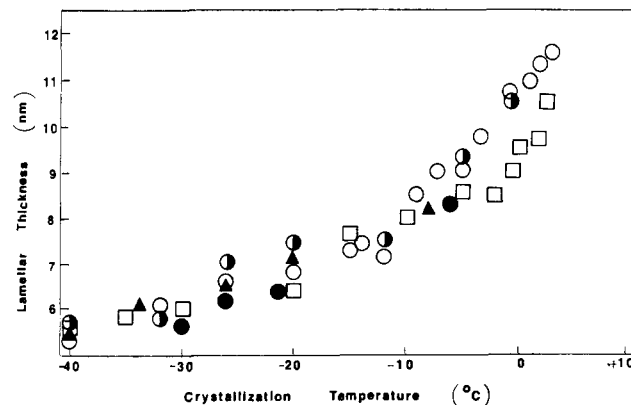


Figure 8. Lamellar thickness as a function of crystallization temperature for the hevea rubber fractions with molecular weights (\circ) 3.13×10^5 , (\bullet) 3.51×10^5 , (\square) 5.43×10^5 , (\blacktriangle) 8.97×10^5 , and (\bullet) 1.42×10^6 .

some lamellae have thickened considerably. The histograms in Figure 7 were obtained from a sampling of 50–60 lamellae in the edge-on orientation in each example. The peak values of lamellar thickness are presented in Figure 8 where it can be seen that all specimens show an increasing lamellar thickness with decreasing supercooling, as expected. Although most of the scatter is within the experimental uncertainty, at higher crystallization temperatures the two lower molecular weight specimens show a clear tendency to produce thicker crystals.

Discussion

The shape of the detailed growth curve of Figure 3 is worthy of attention. Interest lies mainly in the shape of the upper temperature portion ($T_c > -8^\circ\text{C}$) which resembles that reported by Hoffman et al.³ for fractions of polyethylene. The temperature corresponding to the intersection of the approximately horizontal portion with the steeply dropping higher temperature curve corresponds to the aforementioned change in morphology from spherulite to axialite. By analogy with polyethylene, it appears that a regime I–regime II transition is occurring. Additional indirect evidence for this occurrence lies in the variation of branching frequency with crystallization temperature (Figure 9a). It has been observed, but not quantified, that in linear polyethylene²⁰ an increase in branching is observed caused by a preponderance of screw dislocations in the temperature region just below the regime I–regime II transition region. For higher supercoolings in polyethylene the enhanced helicoidal twisting cannot be observed when regular helicoidal twisting appears. Here a similar phenomenon is occurring. A peak in branching frequency can be seen superposed on a general trend of increasing branching frequency with supercooling. The upper and lower temperature bounds of the peak correspond to the proposed regime I–regime II transition temperature and the known regime II–regime III transition temperature. Also plotted is the branching frequency vs. temperature curve of the fraction of molecular weight 543 000. It can be seen that only the upward trend in frequency with increasing supercooling is observed clearly for this fraction which shows only the regime II–regime III transition close to the upper limit of crystallization temperature, although there is a clear but narrow increase in branching frequency just below the transition.

Further evidence for the existence of a regime I region lies in the morphology observed and in the fractionation evident in the formation of both axialites and single crystals. These single crystals are skeletalized, as were those observed earlier in unfractionated *cis*-polyisoprene

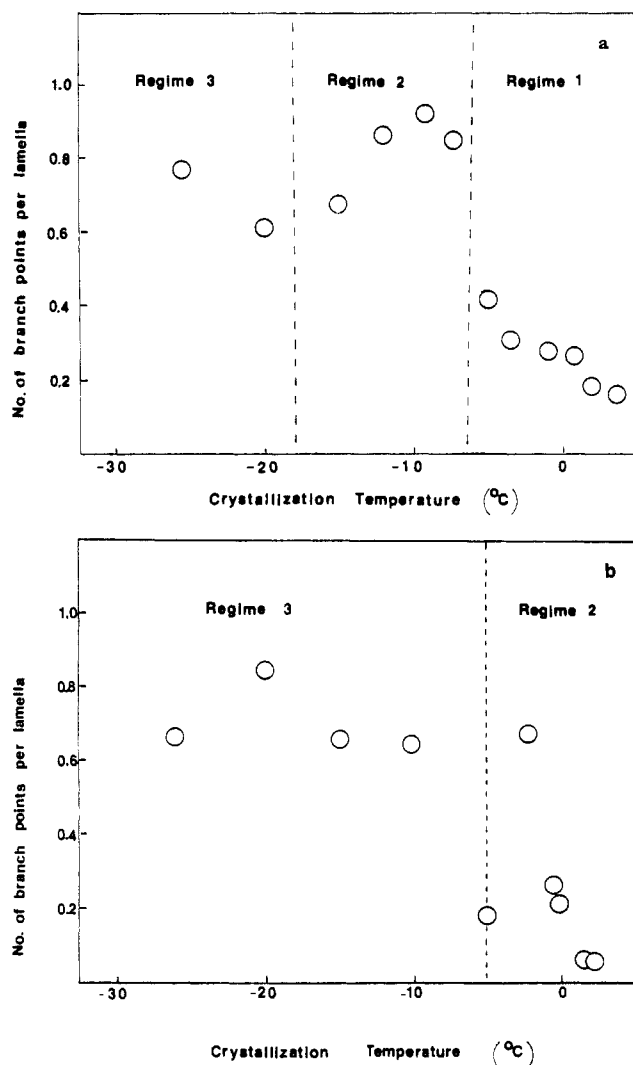


Figure 9. Branching frequency vs. temperature for fractions of molecular weight (a) 3.13×10^5 and (b) 5.43×10^5 .

at elevated pressures.¹⁷ Here the pleats are well defined and it can be seen that each crystal contains a number of central points throughout the skeletalized portion. It is suggested that this is a result of twinning or epitaxy and is responsible for the skeletalized form. Apparently the original crystal was a hollow pyramid which generated additional hollow pyramids but only on one side. Such behavior is well-known in polyethylene single crystals grown from solution. The growth rates of these crystals have not been estimated, but all are fully formed for the shortest times used (25 h at the highest regime I super-coolings).

Analysis of the experimental kinetic data has been carried out by using secondary nucleation theory¹ and identical parameters with those used by Dalal and Phillips⁹ for unfractionated hevea rubber and Rensch et al.¹⁰ for guayule rubber. It will be recalled that the two latter analyses yielded regime II–regime III transitions.

The governing equation relating growth rate to super-cooling is

$$G = G_0 \exp\left(\frac{-U^*}{R(T - T_\infty)}\right) \exp\left(\frac{-Kg}{T(\Delta T)f}\right) \quad (1)$$

where $Kg(\text{regime II}) = 2b\sigma\sigma_e T_m/k\Delta H_f$ and $Kg(\text{regimes I, III}) = 4b\sigma\sigma_e T_m/K\Delta H_f$, T is the crystallization temperature, T_m is the equilibrium melting point, σ is the lateral surface free energy, σ_e is the fold surface free energy, b is the lattice

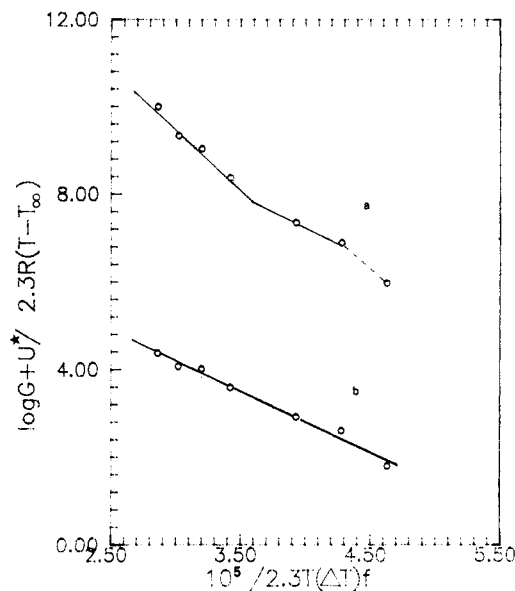


Figure 10. Plot of $\log G + U^*/2.3R(T - T_\infty)$ vs. $1/2.3T(\Delta T)f$ for the hevea rubber fraction of molecular weight 3.51×10^5 .

parameter in the growth direction, and k is the Boltzman constant. f is a parameter correcting the variation in ΔH_f with temperature and put equal to $2T/(T + T_m)$. The first exponential term introduces the mobility, diffusion, or jump rate effect. Two treatments of this term have been used, identical with those of Dalal and Phillips.⁹ In the first treatment values of U^* of 17.2 kJ mol^{-1} and T_∞ of 150.7 K , corresponding to independently determined WLF analyses, were used. In the second the empirical “universal” values of U^* of 6.28 kJ mol^{-1} and T_∞ of 171 K of Hoffman et al.¹ were used. In both cases the experimentally determined¹⁹ equilibrium melting point of 308.7 K was used. It will be recalled that in prior analyses^{9,10} a regime II–regime III transition was observed for unfractionated polymer for WLF analysis but not for the one involving the universal constants. Theory predicts that in a plot of $\log G + U^*/2.3R(T - T_\infty)$ vs. $1/T(\Delta T)f$ a change of slope occurs at the transition and the ratio of the slopes of the regime III to regime II portions should equal 2.0 if there are no changes in the input parameters with regime. In the analyses referred to in ref 9, 10 the slope ratios ranged from 1.65 to 1.83.

The appropriate plots are shown in Figures 10 and 11 for fractions of molecular weight 351 000 and 897 000, respectively. Curve (a) corresponds to the WLF parameter approach and (b) to the universal parameter approach in each case. It can be seen clearly that approach (a) gives rise to two clear transitions for the lower molecular weight fraction but not for the higher molecular weight fraction. The transition occurs at -18.1°C for 3.13×10^5 molecular weight and -17.2°C for 3.51×10^5 . The slope ratios are 1.95 and 1.86, respectively.

Curves for all fractions of molecular weight greater than 897 000 were similar to Figure 11. An upper transition occurs for the lowest molecular weight fraction studied in detail (Figure 12) and the slope ratio for the regime I–regime II transition is 1.86. The upper transition can be defined with some accuracy, independent of curve fitting, because of the observed morphological change. The lower transition is more difficult to define since there is no major morphological effect occurring. Indeed, the transition region is better represented by a curve, such as was noted for poly(phenylene sulfide).¹² The solid line drawn for the lowest temperatures (i.e., the regime III region) represents the lower temperature asymptote independent of the

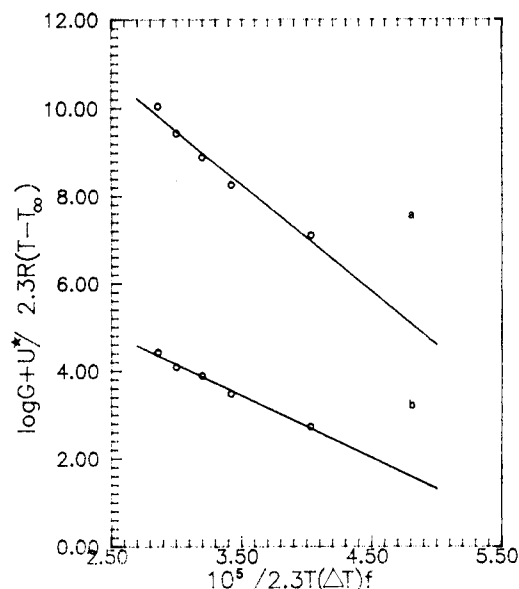


Figure 11. Plot of $\log G + U^*/2.3(T - T_\infty)$ vs. $10^5/2.3T(\Delta T)f$ for the hevea rubber fraction of molecular weight 8.97×10^5 .

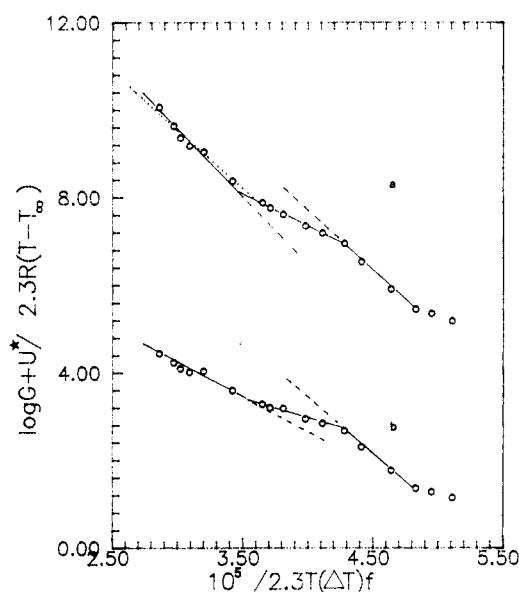


Figure 12. Plot of $\log G + U^*/2.3(T - T_\infty)$ vs. $10^5/2.3T(\Delta T)f$ for the hevea rubber fraction of molecular weight 3.13×10^5 .

curvature. An alternative line having the same linear regression coefficient as the solid line is drawn dotted. For this line, however, the lowest temperature point, which is quite accurate because of the low growth rates involved, is the point left off the line.

The transitions can also be seen in the curves by using analytical approach (b); however, here the slope ratios are 1.5 and 2.5 for the regime II–III and regime I–II transitions, respectively. It had been noted earlier⁴ for polyethylene that the detection of the regime I–II transition is relatively insensitive to the choice of internal diffusional parameters. It has been known for some time that analyses of high supercooling data are very sensitive to mobility parameters.^{9,12} The data points in the regime I region follow the line drawn only for the first few degrees above the regime I–regime II transition. Detailed data for the 543 000 molecular weight fraction are presented in Figure 13 where it can be seen that the regime II–regime III transition occurs at -5°C . A change in molecular weight of less than a factor of 2 has produced an elevation in the transition temperature of 13°C .

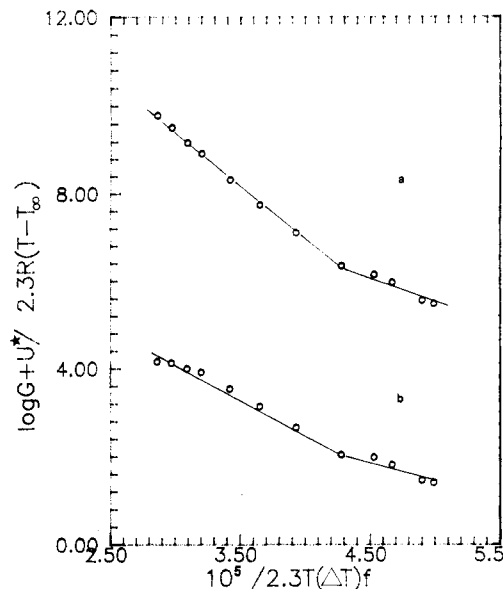


Figure 13. Plot of $\log G + U^*/2.3(T - T_\infty)$ vs. $10^5/2.3T(\Delta T)f$ for the hevea rubber fraction of molecular weight 5.43×10^5 .

The lack of a straight line fit over the entire temperature range above the regime I–regime II transition requires comment. As observed earlier, the regime I temperature range is characterized by molecular weight fractionation. Since the single crystals will be of lowest molecular weight, the remaining axialitic species observed may be of a molecular weight higher than the average. This effect would be intensified as the fraction of single crystals increases at the lowest supercoolings used. It is therefore possible for the molecular weight of the axialitic species to have increased so much that the growth has reverted to regime II. However, there are two other possible explanations. Goldenfeld²¹ has pointed out that regime I growth is itself inherently unstable because as a crystal grows its growth faces will become so extensive that multiple nucleation will be an inevitable result producing a reversion to regime II kinetics. However, for the Goldenfeld explanation to be valid it would be necessary for the reversion to have a temperature dependence; an aspect which has not yet been explored theoretically. Using a different approach involving the influence of surface roughening on substrate completion, Hoffman²² has suggested that regime I should revert to regime II at sufficiently high temperatures. The origin of the observed data can only be resolved by a more in-depth study of growth habits of a much narrower fraction than is currently available.

The results suggest strongly that for any polymer a maximum molecular weight exists beyond which regime II growth will not be observed and that for *cis*-polyisoprene this critical weight is somewhere in excess of 5.4×10^5 . It has been demonstrated¹ that a maximum molecular weight limit of 10^5 exists for polyethylene beyond which regime I growth does not occur. Apparently here the critical molecular weight for regime I is between 3.5 and 5.4×10^5 . It is important to note that three basic types of behavior have been observed here: (a) all three regimes; (b) regimes II and III; (c) only regime III. It is also important to recognize that the slope ratios for all transitions in the fractions are close to the theoretical value of 2.0. Such an observation demonstrates that the molecular weight distribution is critically important to the detection of regime transitions. A broad molecular weight distribution smears the transitions and reduces the slope ratios below the theoretical value. The regime I–regime II transition in polyethylene is also smeared by molecular weight distri-

Table II
Surface Free Energies

MW	regime	kinetics studies			lamellar thickness $\sigma_e, \text{J m}^{-2}$
		Kg	$\sigma\sigma_e, \text{J}^{-2} \text{M}^{-4}$	$\sigma_e, \text{J m}^{-2}$	
3.13×10^5	III	2.87×10^5	3.29×10^{-4}	2.35×10^{-2}	2.62×10^{-2}
	II	1.46×10^5	3.35×10^{-4}	2.39×10^{-2}	
	I	2.71×10^5	3.11×10^{-4}	2.22×10^{-2}	
3.51×10^5	III	2.80×10^5	3.21×10^{-4}	2.29×10^{-2}	2.42×10^{-2}
	II	1.50×10^5	3.44×10^{-4}	2.46×10^{-2}	
	I	2.63×10^5	3.02×10^{-4}	2.16×10^{-2}	
5.43×10^5	III	2.46×10^5	2.82×10^{-4}	2.01×10^{-2}	1.94×10^{-2}
	II	1.28×10^5	2.94×10^{-4}	2.10×10^{-2}	
8.97×10^5	III	2.47×10^5	2.84×10^{-4}	2.03×10^{-2}	1.95×10^{-2}
1.42×10^6	III	2.48×10^5	2.81×10^{-4}	2.01×10^{-2}	1.92×10^{-2}

bution,³ but information is not available regarding its influence on slope ratio. For unfractionated or imperfectly fractionated systems, therefore, the value of the slope ratio cannot be used to optimize curve-fitting procedures, further complicating analyses of crystallization at high supercooling. It is also important to note that in the fraction where both regime transitions occur the sum of the slope ratios is close to 4 regardless of the choice of mobility parameters used in the analysis. Although the WLF approach gave an excellent fit without any attempt at manipulation, if manipulation of the data had been performed so as to produce a slope ratio of 2.0 for regime I–regime II it would also have produced a slope ratio close to 2.0 for regime II–regime III at the same time. In polymers not showing all three regimes it is possible to produce a linear curve indicative of only one regime or “apparent” regime I–regime II or regime II–regime III transitions by appropriate manipulation of mobility parameters. The regime II–regime III transition is especially sensitive to such manipulation. It is important to recognize the significance of the data reported and the analytical method used here in demonstrating (a) the existence of all three regimes in one polymer, (b) the correlation between theoretically predicted slope ratios with the experimental slope ratios determined for transitions, and (c) the effectiveness of the use of WLF parameters, specific to the polymer in question, as mobility parameters in kinetics analysis.

Further quantification of the molecular weight effect can be obtained from a calculation of the fold surface energy, σ_e , by using eq 1. Results are tabulated in Table II where it can be seen that those fractions not showing regime behavior have $\sigma\sigma_e$ values 10% lower than those of the lower molecular weight fractions showing the regime transitions. When converted to σ_e values by using the well-established value of σ equal to $1.4 \times 10^{-2} \text{ J m}^{-2}$ a 10% change in σ_e also results. Presumably this effect is caused by a lower concentration of adjacent reentry folds in the surface of lamellae crystallized in regime III. A test of this conclusion rests on the independent estimation of σ_e from the lamellar thickness supercooling relation.

Use of eq 2, where γ is the thickening ratio, permits such an estimate to be made. Plots of lamellar thickness (l)

$$l = \frac{2Tm^0\sigma_e\gamma}{\Delta H_f\Delta Tf} + l_0 \quad (2)$$

vs. $1/f\Delta T$ are shown in Figure 14 for the two fractions studied in detail. It can be seen that the lower molecular weight fraction shows a slightly higher slope than the higher molecular weight one, although it should be noted that the data for the two fractions are essentially indistinguishable below the regime I–regime II transition ($l \approx$

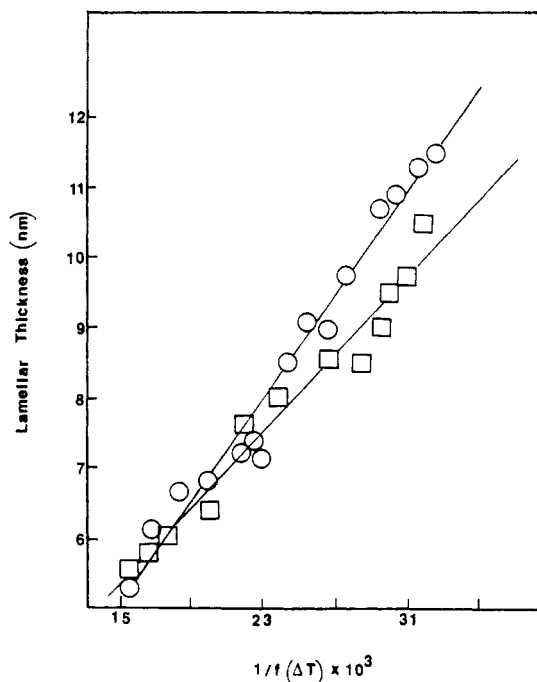


Figure 14. Plot of lamellar thickness vs. $1/10^3(f\Delta T)$ for the hevea rubber fractions having molecular weights (○) 3.13×10^5 and (□) 5.43×10^5 .

85 Å). Calculation of σ_e using a value of γ of 1.46 (9) results in values of σ_e comparable to those obtained from the kinetic data (Table II). Although the errors are sizeable because of the low lamellar thicknesses typical of *cis*-polyisoprene, the effect is clear. Both σ_e values for each fraction differ by no more than 11% whereas the difference between values for the low and high molecular fractions is never less than 15%. The two independent estimations of σ_e therefore correlate as well as can be expected, further confirming the validity of the kinetic analyses.

Regime theory predicts that there will be no change in the lamellar thickness–temperature relation caused by a regime. If, however, there is a change in σ_e accompanying a regime transition, as a result of changes in adjacent reentry folding fractions, the slope of a plot such as that in Figure 14 would be expected to change. We have explored this possibility by simply curve fitting the data for the different regime regions separately. For molecular weight fraction 3.13×10^5 the σ_e values are regime I, $3.3 \times 10^{-2} \text{ J m}^{-2}$; regime II, $3.2 \times 10^{-2} \text{ J m}^{-2}$; and regime III, $2.33 \times 10^{-2} \text{ J m}^{-2}$ and for molecular weight fraction 5.4×10^5 they are, regime II, $2.59 \times 10^{-2} \text{ J m}^{-2}$ and regime III, $2.03 \times 10^{-2} \text{ J m}^{-2}$. Because of the smaller number of points being considered the correlation coefficients were lower,

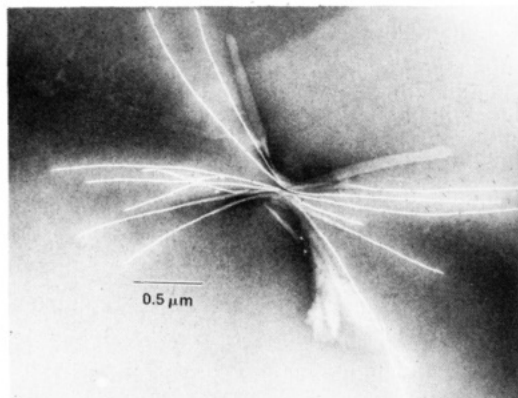


Figure 15. Spherulite axialite showing evidence of fractionated growth in the regime I region ($T_c = -1^\circ\text{C}$).

averaging 0.943, whereas the correlation coefficients for the single continuous fits average 0.984. Although there is some indication of slope change, always in the direction of lower σ_e values for higher supercoolings, the number of points available limit the confidence that can be placed in the analysis.

Some comment should be made on the morphological changes associated with the regime I–regime II transition. In linear polyethylene³ a clear change from axialites in regime I to spherulites in regime II was observed. Here the change is not so dramatic, perhaps because of the molecular weight distribution ($M_w/M_n = 1.5$) being much broader than those of the polyethylene fractions. In both regimes the species begin as sheaves comprising three to seven lamellae. Lamellae growing in regime II, when observed in the “turned-over” orientation, conform to the well-established ribbonlike form having a width of ~ 400 Å. The width increases with crystallization temperature. In regime I the growth is clearly platelike and the lamellar width is of the order of the lamellar length. The growth front, however, remains flat or is curved and does not take on the sharp faceted appearance of single crystals. Evidence for the dependence of lamellar width on regime can be seen in Figure 15 for a crystallization temperature just inside regime I. The lower right part of the aggregate has crystallized in regime I showing very wide lamellae whereas the upper portion exhibits wide ribbons typical of regime II crystallization close to the transition. Presumably the different widths are due to molecular weight fractionation.

The regime II–III transition is believed to be associated with a situation in which the frequency of secondary nucleation exceeds the rate of lateral spreading. Under normal circumstances the rate of lateral growth should be greatest because of the lower energy penalty associated with attachment to a niche on the crystal surface. A strong presumption to be made therefore is that the mobility of lengths of polymer chain greater than the lamellar thickness is significantly impeded under the conditions producing regime III. Mobility will be determined by the internal flexibility of the polymer chain together with the length of the polymer chain. The former is an intrinsic property of the stereochemistry of the chain, the latter a function of the chain's ability to translate over large distances. For instance, cross-linked polyethylene always shows regime III behavior since translation over long distances is not possible.²³ In the case of high molecular weight polymers rheological behavior has often been interpreted by using the concept of “permanent” entanglements. Since the advent of reptation theory,²⁴ however, the concept of permanent entanglements should be replaced with the concept of time scale of chain translation

relative to the time scale of crystallization, except of course for actual knots. A longer chain simply cannot disentangle effectively on the time scale of crystal growth. The critical condition for onset of ineffective disentanglement will be related to both chain length and to the intrinsic flexibility of the polymer chain. For a given molecular weight therefore the onset of ineffective disentanglement will be determined by temperature in a manner similar to the onset of molecular stiffness, i.e., the regime II–regime III transition should be related to the glass transition. The growth curve of Figure 3, as well as the sensitivity of the regime III slope to mobility parameters, demonstrates clearly the importance of internal diffusion in crystallization at high supercoolings. Indeed, the mobility exponential controls the crystallization and the process can be regarded as diffusion controlled. In contrast to the regime I–regime II transition, which is determined by supercooling (i.e., probably thermodynamic in nature) the regime II–regime III transition appears to be controlled by molecular dynamics or at least to have strong molecular dynamic overtones. Such a hypothesis is consistent with current information but must be related in an independent manner. Pressure studies of the regime I–regime II transition in polyethylene⁴ clearly demonstrated its probable thermodynamic origin since the pressure dependence of the regime transition paralleled that of the equilibrium melting point. When the effect of pressure on lamellar growth in unfractionated *cis*-polyisoprene was first reported²⁵ it was noted that single crystals were generated at low supercoolings. Indeed a line was drawn showing the maximum supercooling for single-crystal formation as a function of pressure (see ref 25, Figure 7). That line is now to be identified with the regime I–regime II transition in *cis*-polyisoprene. It also tends to mirror the equilibrium melting line but the correlation must await a detailed evaluation, which will be reported at a later date. Testing of the validity of the kinetic hypothesis of the regime II–regime III transition must await evaluation of its pressure dependence and in particular its relation to the known pressure dependence²⁶ of the glass transition of natural rubber.

An alternative approach to nucleation theory is the new one introducing surface roughening as a substitute for nucleation as the operating mechanism in crystal growth.^{27–29} This approach has not yet been tested quantitatively and is still in its formative stages. We choose not to comment on the validity of the surface-roughening approach at this time. Attempts at its evaluation using the data reported here are under way and will be reported in a separate publication.

Conclusions

- (1) The regime II–regime III and regime I–regime II transitions occur in *cis*-polyisoprene and are molecular weight dependent.
- (2) Fractionated *cis*-polyisoprene of molecular weight 3.13×10^5 shows all three regimes of crystal growth; a fraction of molecular weight 5.4×10^5 shows only regime II and regime III.
- (3) When molecular weight is equal to or exceeds 8.9×10^5 only regime III growth occurs.
- (4) Narrow molecular weight fractions are needed for the ratio of $K_g(\text{III})$ to $K_g(\text{II})$ and of $K_g(\text{I})$ to $K_g(\text{II})$ to equal the theoretical values of 2.0.
- (5) Fold surface free energy is molecular weight dependent, being lower for fractions exhibiting only regime III.
- (6) The regime II–regime III transition is influenced strongly by kinetic effects.

Acknowledgment. This research has been supported by the Polymer Program of the National Science Found-

dation under Grant DMR 83M20212.

References and Notes

- (1) Hoffman, J. D.; Davis, G. T.; Lauritzen, J. I. In *Treatise on Solid State Chemistry*; Hannay, N. B., Ed.; Plenum: New York, 1976; Vol. 3, Chapter 7.
- (2) Lauritzen, J.; Hoffman, J. D. *J. Appl. Phys.* **1973**, *44*, 4340.
- (3) Hoffman, J. D.; Ross, G. S.; Frolen, L.; Lauritzen, J. I. *J. Res. Natl. Bur. Stand., Sect. A* **1975**, *79A*, 671.
- (4) Phillips, P. J.; Tseng, H. T. *Macromolecules*, **1985**, *18*, 1565.
- (5) Vasanthakumari, R.; Pennings, A. J. *Polymer* **1983**, *24*, 175.
- (6) Rensch, G. J.; Taylor, K. D.; Phillips, P. J. *J. Polym. Sci., Polym. Phys. Ed.*, in press.
- (7) Phillips, P. J. *Polym. Prepr. (Am. Chem. Soc., Div. Polym. Chem.)* **1979**, *20*, 438.
- (8) Hoffman, J. D. *Polymer* **1983**, *24*, 3.
- (9) Dalal, E. N.; Phillips, P. J. *J. Polym. Sci., Polym. Phys. Ed.* **1984**, *22*, 7.
- (10) Rensch, P. J.; Phillips, P. J.; Vatansever, N.; Gonzalez, V. J. *Polym. Sci., Polym. Phys. Ed.* **1986**, *24*, 1943.
- (11) Clark, E. J.; Hoffman, J. D. *Macromolecules* **1984**, *17*, 878.
- (12) Lovinger, A. J.; Davis, D. D.; Padden, F. J. *Polymer* **1985**, *26*, 1595.
- (13) Subramaniam, A. *Prepr.—Am. Chem. Soc. Div. Rubber Chem.* **1971**, Paper 78.
- (14) Peachey, L. D. *Proceedings of Fourth International Conference on Electron Microscopy*; Springer Verlag: Berlin, 1958.
- (15) Magill, J. D. *J. Polym. Sci., Part B* **1958**, *6*, 853.
- (16) van Antwerpen, F.; van Krevelen, D. W. *J. Polym. Sci., Polym. Phys. Ed.* **1972**, *10*, 2423.
- (17) Edwards, B. C.; Phillips, P. J. *J. Polym. Sci., Polym. Phys. Ed.* **1976**, *14*, 391.
- (18) Davies, C. K. L.; Ong, E. L. *J. Mater. Sci.* **1977**, *12*, 2165.
- (19) Dalal, E. N.; Taylor, K. D.; Phillips, P. J. *Polymer* **1983**, *24*, 1623.
- (20) Phillips, P. J.; Philpot, R. *Polym. Commun.* **1986**, *27*, 307.
- (21) Goldenfeld, N. *Polym. Commun.* **1984**, *25*, 47.
- (22) Hoffman, J. D. *Polymer* **1985**, *26*, 1763.
- (23) Phillips, P. J.; Kao, Y. H. *Polymer*, **1986**, *27*, 1679.
- (24) de Gennes, P.-G. *Scaling Concepts in Polymer Physics*; Cornell University: Ithaca, NY, 1979.
- (25) Phillips, P. J.; Edwards, B. C. *J. Polym. Sci., Polym. Phys. Ed.* **1975**, *13*, 1819.
- (26) Dalal, E. N.; Phillips, P. J. *Macromolecules* **1983**, *16*, 890.
- (27) Sadler, D. M.; Gilmer, G. H. *Polymer* **1984**, *25*, 1446.
- (28) Sadler, D. M.; Gilmer, G. H. *Phys. Rev. Lett.* **1986**, *56*, 2708.
- (29) Sadler, D. M. *Polym. Commun.* **1986**, *27*, 143.

Reversible Swelling of Gel-Like Silica-Filled Siloxanes. NMR Approach to Static Scaling Properties

J. P. Cohen-Addad,* A. Viallat, and P. Huchot

Laboratoire de Spectrométrie Physique associé au CNRS, Université Scientifique, Technologique et Médicale de Grenoble, B.P. 87-38402 St. Martin d'Heres, Cedex, France.
Received October 6, 1986

ABSTRACT: This work deals with the gel-like behavior of systems resulting from mechanical mixing of high molecular weight siloxane chains with silica particles. Statistical properties of polymer chains were probed by measurement of the magnetic relaxation of protons after removing all free siloxane chains. The specific residual amount of polymer bound to silica was varied from 1.2 to 2.4 (w/w); the fractal character of siloxane chains bridging particles and dangling chains was enhanced by using a swelling agent (chloroform). The spin-lattice relaxation of protons was shown to be insensitive to silica concentration variations; it was also insensitive to the addition of solvent, at polymer concentrations smaller than about 2.4 (w/w). These two results were assigned to the presence of dynamic screening domains analogous to those originating from entanglements in a pure melt. Scaling properties of these domains were probed in a semilocal space scale from the transverse magnetic relaxation of protons. Results observed in these systems are in very strong contrast to those observed for calibrated gels: (a) no packing condition effect was observed and (b) no affine property was induced by reversibly swelling silica-filled siloxane systems.

I. Introduction

This work describes an NMR investigation attempting to characterize the unfolding mechanism of polymer chains in a gel-like structure, i.e., a system where mineral filler particles serve the function of interlinkages; in addition to these junctions, physical combinations of chains are also mediated by trapped entanglements. The present study concerns siloxane chains linked to silica particles through hydrogen bonding; the size and the concentration of silica particles, on the one hand, and the average chain molecular weight, on the other hand, were chosen in a way appropriate to the formation of a network structure. The unfolding effect of polymer chains connecting silica particles was induced by a swelling agent. Although siloxane chains are not covalently linked to particles, the random mixture resulting from a saturated adsorption onto the silica surface may be reversibly swollen by using a suitably good solvent. The mixture may be shown to behave like a permanent gel because interlinkages provided by hydrogen bonds are strong compared with the strength of silica-solvent interactions.

It has been long recognized that elementary chains in a gel have a fractal character: they store the elastic energy of the system. Also, the statistical volume pervaded by a given elementary chain is much larger than the volume

of the corresponding condensed material.¹ Polymer chains are known to be swollen by one another in a pure melt. Elementary chains in a gel are likewise intertwined, notwithstanding the presence of cross-links.² The collective fractal character of a gel can be perceived from its elastic equation of state,³ whereas the individual fractal character of elementary chains cannot be observed without contrasting some of them with neighboring chains which serve the function of a swelling agent.

The contrast may be created by a partial deuteration of the network.² This labeled system has been used to illustrate a fundamental property of polymeric gels: the mean square dimension of the chain segment joining two successive covalent links is governed by Gaussian statistics. It is equal to that measured from a similar chain segment embedded in a pure melt. The observation of swelling effects of a network structure is a convenient way often used to explore gel properties because it magnifies the fractal character of elementary chains. The maximum swelling, obtained at equilibrium with a pure solvent, reflects the full unfolding of elementary chains taking excluded volume effects into consideration.⁴ The maximum swelling effect obeys the C*-theorem propounded by De Gennes. Correspondingly, the elastic modulus of a swollen gel is weakened.⁴ However, it may be worth emphasizing